Correlation between DSC Curves and Isobaric State Diagrams. 3. Simulation of Smeared DSC Curves

Andreas Müller and Werner Borchard*

Angewandte Physikalische Chemie, Gerhard-Mercator-Universität Duisburg, Lotharstrasse 1, D-47048 Duisburg, Germany

Received: November 13, 1996; In Final Form: March 4, 1997[⊗]

Using *n*-hexane (*n*-C_6H_{14}) and *n*-dodecane (*n*-$C_{12}H_{26}$) as a binary model system, the smearing of isobaric DSC curves, which is a result of a limited heat flow in the calorimeter, is the subject of the present paper. The underlying heat conduction process notwithstanding, the method introduced allows one to simulate the smeared traces of real isobaric DSC curves of binary systems by superimposing a large number of Gaussian curves. The resulting curves have proved to be in good agreement with the experimental data.

1. Introduction

Several formulas of utmost generality have been derived that in principle describe the trace of a $\tilde{c}_P(T)$ curve (DSC curve) straight through an isobaric binary state diagram while performing a scan on a differential scanning calorimeter (DSC).[1] These relationships permit calculating an isobaric DSC curve from any phase diagram, however, under the condition that a continuous phase transition takes place which should be completed within a DSC measurement; additionally, the eutectic enthalpies of fusion at the eutectic temperature which pertain to an invariant first-order transition according to Ehrenfest[2] have also been described quantitatively. However, all formulas derived refer to real equilibrium states at any time; that is, it has been disregarded hitherto that the calculated $\tilde{c}_P(T)$ curves do not exactly reflect the proper intermediate phases traversed due to a time delay that is a consequence of transport phenomena such as diffusion or heat exchange. This time delay termed "smearing"[3] usually leads to a certain peak broadening of every transition peak recorded by DSC. For this reason, the experimental DSC curves of the model system investigated, *n*-hexane (*n*-C_6H_{14}) and *n*-dodecane (*n*-$C_{12}H_{26}$), have proved to be somewhat broadened and flatter with respect to the calculated ones.[1]

In accordance with the relations derived,[4,5] the left-hand side of any sharp melting peak should ascend linearly, such as the melting peak of a eutectic mixture and that of a pure crystal. On passing the peak maximum, the right-hand side of this peak decreases exponentially.[4,6] In effect, the shapes of real melting peaks bear a strong resemblance to Gaussian curves showing, however, a slight asymmetry. That is why the eutectic peaks—which should, in thermodynamic terms, represent infinitely sharp fusion peaks with infinite peak heights—have already been fitted by means of Gaussian curves to render them depictable on a graph, but also to fit them to experimental conditions where finite peak widths and heights are observed anyway.[1] Yet the experimental eutectic peaks turned out not to be well-reproduced since their widths have been fitted to those of the pure components, although, indeed, they alter depending on the initial composition w_2^o.

In the present paper, it is our objective to simulate the "smeared" traces of real DSC curves of the underlying model system, *n*-C_6H_{14}/*n*-$C_{12}H_{26}$, equivalent to that of the preceding paper.[1] With this aim in view, the eutectic peak widths are to be fitted by a Gaussian distribution of which the widths will be estimated pursuant to the relations derived in the preceding paper.[5] Moreover the fusion peak of the pure *n*-dodecane (λ-transition peak[1,7]), following the eutectic transition and ranging from the eutectic temperature T_E to the liquidus (or melting) temperature T_m (see Figure 1), is to be simulated by superimposing a multitude of Gaussian curves regardless of the underlying mechanism of heat conduction in the course of the DSC scan. The areas of the Gaussian curves are hereby to be assigned to the respective enthalpies at every temperature, while the widths are always equated to those of the pure components. In the end, the asymmetry of the real melting peaks will be taken into account in a second approach.

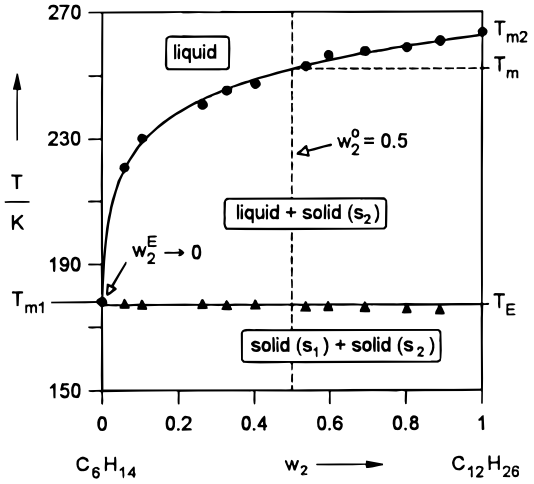

Figure 1. Isobaric eutectic state diagram of the binary system *n*-hexane (*n*-C_6H_{14})/*n*-dodecane (*n*-$C_{12}H_{26}$) with the liquidus temperatures T_m (●) and the eutectic temperatures T_E (▲) plotted against the mass fraction w_2. T_{m1} and T_{m2}: melting temperatures of the pure hexane and dodecane. Dashed vertical line: trace of the DSC scan straight through the state diagram for an initial concentration of $w_2^o = 0.5$ (see text).

2. Simulation of the "Smeared" DSC Curves

Since the underlying model system in Figure 1, consisting of *n*-hexane (component 1) and *n*-dodecane (component 2), does not reveal any solid solution behavior, the specific eutectic enthalpy of fusion, $\Delta\tilde{H}_E$, is given by the identity[1]

* To whom correspondence should be addressed.

[⊗] Abstract published in *Advance ACS Abstracts,* April 15, 1997.

S1089-5647(96)03783-2 CCC: $14.00

$$\Delta\tilde{H}_E = \frac{1 - w_2^o}{1 - w_2^E}\cdot[(1 - w_2^E)\cdot\Delta\tilde{H}_{01} + w_2^E\cdot\Delta\tilde{H}_{02} + \Delta\tilde{H}_{mix}^E] \quad (1)$$

Here, w_2^o and w_2^E are the initial composition (overall composition) and the eutectic composition in the mass fraction scale; $\Delta\tilde{H}_{01}$ and $\Delta\tilde{H}_{02}$ denote the specific enthalpies of fusion of the pure *n*-hexane and *n*-dodecane, and $\Delta\tilde{H}_{mix}^E$ is the specific enthalpy of mixing at the eutectic point characterized by the eutectic temperature, T_E, and the eutectic composition, w_2^E. As can be seen from Figure 1, the eutectic composition is shifted toward lower concentrations to such an extent that the eutectic point and the melting point of *n*-hexane are almost coincident (i.e. $w_2^E \rightarrow 0$). Equation 1 therefore applies only to the case $w_2^E \leq w_2^o < 1$.

As reported in our last paper,[5] the width of the eutectic peak is determined by

$$\Delta T_E = \sqrt{\Delta\tilde{H}_E\cdot m\cdot\dot{T}_P\cdot[2\cdot(R_0 + R_I) + R_{II}] + (\dot{T}_P\cdot t_0)^2} \quad (2a)$$

where

$$R_I = m\cdot\frac{w_2^o - w_2^E}{1 - w_2^E}\frac{1}{A^2\cdot\lambda_I\cdot\rho_I} \quad (2b)$$

and

$$R_{II} = m\cdot\frac{1 - w_2^o}{1 - w_2^E}\frac{1}{A^2\cdot\lambda_{II}\cdot\rho_{II}} \quad (2c)$$

Equation 2a characterizes the width of a eutectic peak (ΔT_E) at the foot points thereof. Clearly, ΔT_E depends on the specific eutectic enthalpy of fusion $\Delta\tilde{H}_E$, the total mass of the sample m, the preset heating rate of the calorimeter $\dot{T}_P$, at which the DSC scan is carried out, and the thermal resistances R_0, R_I, and R_{II}. Resistance R_0 hereby refers to the sample-holder and the sample-container, while R_I and R_{II} given by eq 2b and eq 2c are the resistances of the pure solid *n*-dodecane or the liquid eutectic that mainly consists of the liquid *n*-hexane (see Figure 1). Correspondingly, subscripts (I) and (II), appended to the thermal conductivity λ and the density ρ, relate to the crystalline dodecane and the melted hexane. Time t_0 designating the period of time until the proper eutectic transition commences is, however, elusive and may only be achieved by estimation.[5] It must be observed here that t_0 is related to time $t = 0$ as a relative zero, indicating the moment at which the heat source of the calorimeter arrives at temperature T_E. Furthermore, A is the cross-sectional area of the sample and corresponds to the inner diameter of the sample-container. With these relationships at hand, we are thus capable of simulating a real, smeared eutectic peak by use of a Gaussian curve of which the width at its foot point refers to ΔT_E and the peak area is equivalent to $\Delta\tilde{H}_E$.

The fusion peak of the pure dodecane following the eutectic transition within the range between the eutectic temperature and the liquidus temperature (λ-transition) is represented by the expression[1]

$$\tilde{c}_P(T) = \tilde{c}_P^{base}(T) + \tilde{c}_P^{melt}(T) \quad (3a)$$

which comprises the contribution of the base line,

$$\tilde{c}_P^{base}(T) = \frac{1 - w_2^o}{1 - w_2^l}\cdot\left[(1 - w_2^l)\cdot\tilde{c}_{P_{01}}^l + w_2^l\cdot\tilde{c}_{P_{02}}^l + \left(\frac{\partial\Delta\tilde{H}_{mix}^l}{\partial T}\right)_P\right] + \frac{w_2^o - w_2^l}{1 - w_2^l}\cdot\tilde{c}_{P_{02}}^s \quad (3b)$$

and the contribution of a certain amount of the crystal that is subject to fusion at the prevailing temperature T,

$$\tilde{c}_P^{melt}(T) = \frac{1 - w_2^o}{(1 - w_2^l)^2}\cdot\left(\frac{\partial w_2^l}{\partial T}\right)_P\cdot[\Delta\tilde{H}_{02} + \Delta\tilde{H}_{mix}^l] \quad (3c)$$

The subscripts (1) and (2) correspond, as stipulated above, to component 1 (*n*-hexane) and component 2 (*n*-dodecane), whereas the superscripts (s) and (l) denote the quantities assigned to the liquid or solid state, respectively. Furthermore, $\tilde{c}_{P_{01}}^l$ and $\tilde{c}_{P_{02}}^l$ are the specific heat capacities of the pure liquid *n*-hexane and *n*-dodecane, $\tilde{c}_{P_{02}}^s$ is the heat capacity of the pure solid dodecane, $\Delta\tilde{H}_{mix}^l$ is the enthalpy of mixing at the prevailing composition w_2^l of the melt, negligible with respect to $\Delta\tilde{H}_{02}$, and $(\partial w_2^l/\partial T)_P$ is the reciprocal slope of the liquidus curve.[1] This quantity required for calculation of the DSC curves has been taken from the respective phase diagram depicted in Figure 1. Equations 3a−3c are, strictly speaking, applicable only to binary mixtures; for pure substances, w_2^l equals $w_2^o = 0$ or 1, respectively, leading to an infinitely sharp melting peak of which the height becomes infinite ($\tilde{c}_P(T) \rightarrow \infty$).

The specific heat capacities of the solid state (γ = s) prior to the eutectic transition of fusion ($T < T_E$) and of the liquid state (γ = l) subsequent to fusion ($T > T_m$) have been achieved by applying the relation

$$\tilde{c}_P^\gamma(T) = (1 - w_2^o)\cdot\tilde{c}_{P_{01}}^\gamma + w_2^o\cdot\tilde{c}_{P_{02}}^\gamma + \left[\frac{\partial\Delta\tilde{H}_{mix}^\gamma}{\partial T}\right]_P \quad (4)$$

to the relevant state γ.[1] Hence, all $\tilde{c}_P(T)$ curves, computed by means of a total of about 1000−1500 data points (P_i), have thus been assembled by four temperature ranges,[1] namely, those assigned to $T < T_E$ (eq 4), the eutectic transition itself at $T = T_E$ (eq 1), the transition of fusion ranging from T_E to T_m (eqs 3), and the temperature range of the molten sample from $T = T_m$ up to the final temperature of the DSC curve (eq 4).

Integration of the $\tilde{c}_P^{melt}(T)$ curve within the limits between T_E and T_m affords the total specific enthalpy of fusion, $\Delta\tilde{H}$, of the remaining pure crystal of component 2 (*n*-dodecane). This range of fusion may additionally be divided into $(N - 1)$ small intervals, each of which is located between two successive data points P_i and P_{i+1} at the temperatures T_i and T_{i+1}. This means that the total area beneath the $\tilde{c}_P^{melt}(T)$ curve (between T_E and T_m) may be considered to be cut up into a multitude of thin slices whose widths are given by the identity

$$\Delta T_i = T_{i+1} - T_i \quad (i = 1, 2, ..., N) \quad (5a)$$

Consequently, every individual interval between T_i and T_{i+1} possesses a definite amount of enthalpy of fusion, $\Delta\tilde{H}_i$, such that $\Delta\tilde{H} = \sum_{i=1}^N \Delta\tilde{H}_i$, whereby

$$\Delta\tilde{H}_i = \int_{T_i}^{T_{i+1}}\tilde{c}_P^{melt}\,dT \approx \frac{\tilde{c}_P^{melt}(T_{i+1}) + \tilde{c}_P^{melt}(T_i)}{2}\cdot\Delta T_i \quad (5b)$$

In the following, every individual enthalpy $\Delta\tilde{H}_i$ of the respective

intervals ranging from T_i to T_{i+1} is to be assigned to a Gaussian curve considered to commence at temperature T_i:

$$\tilde{c}_{P,i}(T) = \tilde{c}_{P,i}^{\max} \cdot \exp\left[-0.5 \cdot \frac{(T - T_i^{\max})^2}{\sigma^2}\right] \quad (6a)$$

Here, $\tilde{c}_{P,i}^{\max}$ denotes the maximum value of the function located at the temperature $T_i^{\max}$, and σ, called the standard deviation of a Gaussian distribution, is the distance between the point of inflexion and $T_i^{\max}$ (see Figure 2a). In our first approach of simulating "smeared" DSC curves, σ is to be taken from a mean σ of the fusion peaks of the two pure components, *n*-hexane and *n*-dodecane, while its height and therefore its area correspond to $\Delta\tilde{H}_i$, as already outlined above.

For practical purposes, we intend to find a relationship between the standard deviation, σ, the peak height, $\tilde{c}_{P,i}^{\max}$, and the peak width at the *foot* of the Gaussian curve, ΔT, and also the curve area being synonymous with the enthalpy $\Delta\tilde{H}_i$ of the relevant interval between T_i and T_{i+1}. To this end, we integrate a Gaussian curve given by eq 6a by equating those $\tilde{c}_{P,i}(T)$ values to zero whose magnitudes are smaller than an *arbitrarily* defined lower limit of 0.5% related to the maximum $\tilde{c}_{P,i}^{\max}$ involved (so-called "truncated" Gaussian curve). This means that every underlying Gaussian curve may now be considered to be limited by a lower and an upper bound, temperature T_i and temperature T_i*, while the areas beyond these bounds (i.e. for $T < T_i$ and $T > T_i$*) are disregarded, corresponding to a relative error of about 1.25%. As the distances between temperature $T_i^{\max}$ and the onset of the Gaussian curve, T_i, and between temperature $T_i^{\max}$ and the end, T_i*, amount to $3.3 \cdot \sigma$ (this value results from combining eq 6a with the above condition $\tilde{c}_{P,i}(T) = 0.005\tilde{c}_{P,i}^{\max}$, and solving for T_i, $T_i = T_i^{\max} - \sqrt{-2\ln 0.005}\sigma$, and $T_i^* = T_i^{\max} + \sqrt{-2\ln 0.005}\sigma$, respectively),

$$T_i^{\max} = T_i + 3.3 \cdot \sigma = T_i^* - 3.3 \cdot \sigma \quad (6b)$$

the peak width at the *foot* of the Gaussian curve, ΔT, hence reads (see Figure 2a)

$$\Delta T = T_i^* - T_i = 6.6 \cdot \sigma \quad (6c)$$

Relating the area of the Gaussian curve within the limits T_i and T_i* (which is identical with the enthalpy $\Delta\tilde{H}_i$ of the interval between T_i and T_{i+1}) to the maximum height of the curve ($\tilde{c}_{P,i}^{\max}$) furnishes the identity

$$\Delta\tilde{H}_i = \int_{T_i}^{T_i^*} \tilde{c}_{P,i}(T)\, \mathrm{d}T = 2.51 \cdot \sigma \cdot \tilde{c}_{P,i}^{\max} \quad (6d)$$

whereby 2.51σ constitutes the constant of proportionality (in kelvin) of which the factor 2.51 is the reciprocal value of the factor 0.399 given in Figure 2a.

It should be stressed here that ΔT_i must not be confused with ΔT or σ (see eqs 5a and 6c and also Figure 2a): whereas ΔT_i denotes the distance between two successive data points P_{i-1} and P_i of the already calculated ("nonsmeared") DSC curve (see Figure 2c), ΔT is understood to be the constant peak width at the *foot* of every Gaussian curve. Drawing a comparison to ΔT, σ does represent a measure of peak width as well, but it is less suitable for experimental purposes since σ corresponds to half the peak width of a Gaussian curve at a height of about 60.7% related to the maximum peak height $\tilde{c}_{P,i}^{\max}$ (see Figure 2a, as well as eq 6a, with T and $T_i^{\max}$ taken to be σ and 0, respectively).

As every Gaussian curve starts at temperature T_i, and ΔT exceeds ΔT_i by a large scale (i.e. $\Delta T \gg \Delta T_i$), a superimposition of the Gaussian curves will be observed inevitably. Taking the sum of all Gaussian curves at the relevant temperatures T pursuant to

$$\tilde{c}_P^{\mathrm{melt}}(T) = \sum_{i=1}^{N} \tilde{c}_{P,i}(T) = \sum_{i=1}^{N} \tilde{c}_{P,i}^{\max} \exp\left[-0.5 \cdot \frac{(T - T_i^{\max})^2}{\sigma^2}\right] \quad (7)$$

therefore furnishes a DSC curve with a "smeared" fusion peak of which the melting point T_m or the end of fusion, however, is shifted toward higher temperatures, in fact toward $T_m + \Delta T$. This requires compressing the broadened temperature range from $[T_E; T_m + \Delta T]$ to $[T_E; T_m]$. As, however, the peak area will be decreased at the same time, the DSC curve has to be stretched by a certain extent with respect to the ordinate in order to retain the original peak area, i.e. the total enthalpy of fusion of the remaining crystal, $\Delta\tilde{H}$. Consequently, the Gaussian curves cannot all possess the initial peak width ΔT any longer while being superimposed, but are slightly diminished in width by the factor

$$\frac{T_m - T_E}{T_m + \Delta T - T_E} \quad (8a)$$

Superimposing the Gaussian curves hence proceeds as follows: After having established the effective peak width at the foot points pursuant to the relation

$$\Delta T_{\mathrm{eff}} = \frac{T_m - T_E}{T_m + \Delta T - T_E} \cdot \Delta T \quad (8b)$$

we set about determining the effective standard deviation, σ_{eff}, from eq 6c, substituting ΔT_{eff} for ΔT. This, in turn, serves to alter the maximum peak heights of every individual Gaussian curve $\tilde{c}_{P,i}^{\max}$, according to eq 6d, replacing σ by σ_{eff}.

By use of these (modified) Gaussian curves calculated from eq 6a by means of the modified maximum peak heights and the standard deviations σ_{eff}, superimposition now leads to a curve that provides the final "smeared" $\tilde{c}_P^{\mathrm{melt}}(T)$ curve if the temperature range between T_E and $T_m + \Delta T_{\mathrm{eff}}$ is additionally compressed again from $[T_E; T_m + \Delta T_{\mathrm{eff}}]$ to $[T_E; T_m]$ according to the linear relationship

$$T^* = \frac{T_m - T_E}{T_m + \Delta T_{\mathrm{eff}} - T_E} \cdot (T - T_E) + T_E \quad (8c)$$

in order to restore the DSC curve to its original peak area and its real melting interval ranging from T_E to T_m. Here, the asterisk (*) indicates all the temperatures of the compressed temperature scale after transformation. Finally, by summing up the "smeared" $\tilde{c}_P^{\mathrm{melt}}(T)$ curve and the contribution of the original base line (i.e. the $\tilde{c}_P^{\mathrm{base}}(T)$ curve calculated by eq 3b), the desired computed DSC curve showing a "smeared" fusion peak within the temperature range between T_E and T_m will be obtained. It is important to observe that the simulated eutectic fusion peak, which represents a "smearing" as well, proceeds from a single Gaussian curve whose maximum peak height has been obtained by eqs 6d and 1 whereby $\Delta\tilde{H}_i = \Delta\tilde{H}_E$.

A second proposal for simulating "smeared" DSC curves involves the asymmetry of the real, i.e. experimentally obtained, peaks of fusion of the pure components. Strictly speaking, they do not obey a Gaussian distribution because their ascending branches show much smaller absolute values in their slopes than the descending branches (Figure 2a). Clearly, shape and

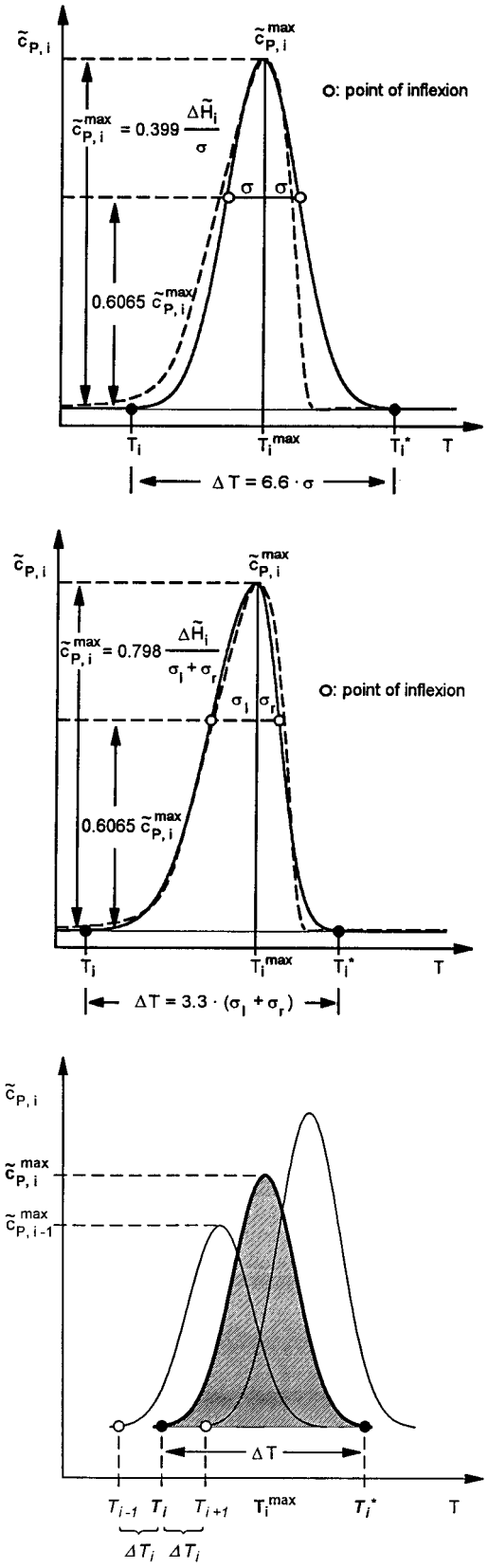

Figure 2. (a, top) Fusion peak of a pure sample (dotted line) fitted by a Gaussian curve (solid line) using a single parameter σ. T_i: onset of the Gaussian curve. T_i*: end of the Gaussian curve. ΔT: peak width at the foot (see text). (b, middle) Fusion peak of a pure sample (dotted line) fitted by a Gaussian curve (solid line) by means of two parameters σ_l and σ_r. T_i: onset of the Gaussian curve. T_i*: end of the Gaussian curve. ΔT: peak width at the foot (see text). (c, bottom) Schematic diagram of three successive Gaussian curves commencing at T_{i-1}, T_i, or T_{i+1}, respectively. ΔT_i: distance between two successive data points. ΔT: peak width at the foot. Hatching: peak area of the ith Gaussian curve (see text).

appearance of the underlying Gaussian curves may be adjusted much more appropriately to the real fusion peaks by introducing two different standard deviations σ_l and σ_r into the eqs 6 and 7, whereby $2\sigma = \sigma_l + \sigma_r$ (Figure 2b). This means that the melting peak is now considered to be split up into a left-hand and a right-hand side, of which the "left" (ascending) branch of the peak is characterized by σ_l and the "right" (descending) branch by σ_r. As a result, there are two cases that need to be distinguished in eqs 6 and 7:

$$T < T_i^{\max}: \quad \Rightarrow \sigma = \sigma_l \tag{9a}$$

$$T > T_i^{\max}: \quad \Rightarrow \sigma = \sigma_r \tag{9b}$$

All other ensuing steps, for instance the superimposition of the Gaussian curves or the transformation and reverse transformation of the temperature scale (eqs 8), proceed in the same manner as already described above in the first approach for a single parameter σ only.

3. Results and Discussion

Figures 3 and 4 demonstrate the simulated smeared DSC curves (solid lines) for four different initial concentrations w_2^o, actually 0.104, 0.400, 0.593, and 0.800. Since faithful experimental data of the specific heat capacities necessary for the calculations (eqs 3 and 4) were not available, neither by our calorimetric measurements nor by any literary reference, we assigned the specific standard heat capacities of *n*-hexane and *n*-dodecane,[8] referred to a unit pressure of 1 atm (1.013 bar) and a temperature of 298 K, to $\tilde{c}^{l}_{P_{01}}$ and $\tilde{c}^{l}_{P_{02}}$,

$$\tilde{c}^{l}_{P_{01}} = 2.27 \text{ J·(g·K)}^{-1}$$

$$\tilde{c}^{l}_{P_{02}} = 2.21 \text{ J·(g·K)}^{-1} \tag{10a}$$

whereas $\tilde{c}^{s}_{P_{01}}$ and $\tilde{c}^{s}_{P_{02}}$ were arbitrarily set to

$$\tilde{c}^{s}_{P_{01}} = 0.27 \text{ J·(g·K)}^{-1}$$

$$\tilde{c}^{s}_{P_{02}} = 0.21 \text{ J·(g·K)}^{-1} \tag{10b}$$

corresponding to a step in the specific heat capacities of 2 J·(g·K)$^{-1}$ at the respective melting point.[1] Furthermore, their temperature-dependence could not be established either, which led us to assume constant heat capacities $\tilde{c}^{\gamma}_{P_{0i}}$ (γ = s, l; i = 1, 2) throughout the entire temperature range. As a result, the computed DSC curves do not reveal any inclination at all. For the sake of a better comparability the original (i.e. experimental) DSC curves indicated by dashed lines in Figures 3 and 4 have thus been tilted by subtraction of a straight line. Additionally each diagram contains an enlargement of the fusion peak at its maximum height.

Within the temperature range of the λ-transition ($T_E < T < T_m$), the fusion peaks of the simulated DSC curves of Figures 3 or 4 are based on the Gaussian curves such as depicted in parts a or b of Figure 2, respectively. Here, the dashed line constitutes the melting peak of *n*-hexane as an example, while the solid line corresponds to the respective Gaussian curve that has been fitted to the experimental peak of fusion under conservation of the total specific enthalpy of fusion.

Figure 2a represents the underlying (symmetrical) Gaussian curve in the first approach of simulating a "smeared" DSC curve in which only a single value of the standard deviation σ has been taken for fitting both the left-hand and the right-hand side

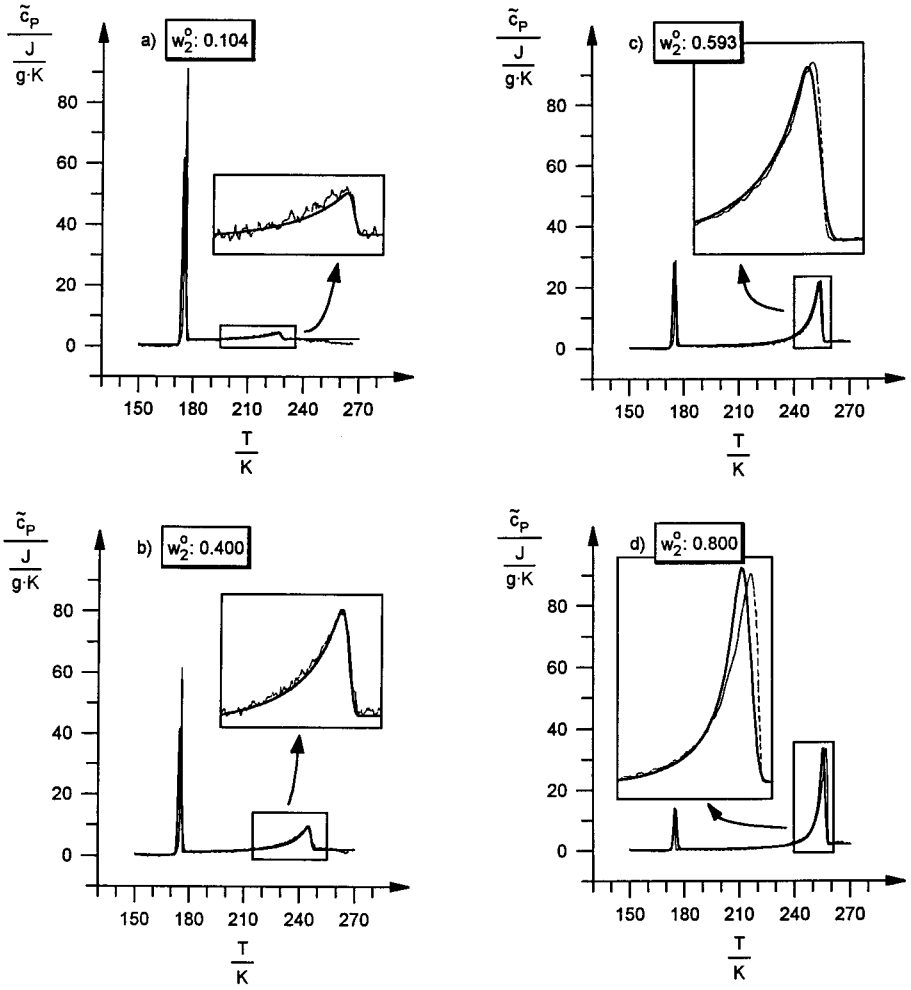

Figure 3. Diagram showing the simulated DSC curves (solid) and the measured DSC curves (dashed) at four different initial compositions calculated by using a single σ parameter only. The narrow peaks at $T < T_E = 178$ K are the eutectic peaks; the broadened peaks at $T > 178$ K correspond to the fusion of the remaining crystal (see text).

of the experimental peak of fusion. Clearly, onset (T_i) and end (T_i*) of the Gaussian curve do not match those of the experimental curve. Or conversely, if onsets and ends of both curves are coincident, their maxima do not concur any longer, whereby the maximum of the Gaussian curve will be shifted toward lower temperatures. This in turn brings about smeared DSC curves in Figure 3 that do not reflect exactly the course of the experimental curves because the maxima of their fusion peaks are similarly shifted toward lower temperatures.

In contrast, Figure 2b depicts the Gaussian curve utilized in our second approach. Here, two different standard deviations σ have been introduced to describe the left-hand and the right-hand side of the underlying fusion peak separately. As can be seen there, σ_l now represents two-thirds of the total peak width (i.e. σ_l:σ_r = 2:1), which permits a satisfactory characterization of the experimental fusion peak. Only the descending branch of the Gaussian curve differs slightly, resulting in a marginal temperature shift of T_i* (by about 0.75 K) with respect to the end of the experimental fusion peak, which corresponds to the melting point of *n*-hexane.

Inspection of Figure 4 reveals that the original curves are relatively well reproduced compared with those of Figure 3, first and foremost with regard to the locus and the height of the maxima of the fusion peaks. Only the last curve of Figure 4d ($w_2^o = 0.8$) shows a marginal shift of the end of fusion toward higher temperatures (by approximately 1.1 K), which is, as already mentioned, a consequence of the minor difference between T_i* and the melting point of the underlying fusion peak (see Figure 2b). Nevertheless this method of simulating smeared DSC curves would probably be improved by using a Fourier series instead of Gaussian curves since the former facilitates tracing any asymmetry of the fusion peak in question. Applying the Fourier series, however, seems to be more laborious than superimposing Gaussian curves.

Finally, it should be noted that the eutectic peaks (sharp peaks at $T < 178$ K) in Figure 3 show certain deviations in widths and heights, which is a consequence of using a single σ parameter only. The computed eutectic peaks in Figure 4, however, coincide with the experimental ones for the most part—except for the last case in Figure 4d—due to the "asymmetric" Gaussian curves taken as a basis. That is, two σ parameters have been used for characterizing the Gaussian curves in question, whose peak widths have additionally been estimated from eq 2a. Owing to a larger mass of the fourth sample ($w_2^o = 0.8$) with respect to the average mass of the underlying system that served the determination of the eutectic peak width according to eq 2a, a narrowed eutectic peak was furnished, as depicted in Figure 4d, leading to a somewhat higher peak with regard to the real one.

4. Conclusions

Experimental DSC curves have proved to be broadened to a certain extent with respect to those calculated.[1] This effect called "smearing"[3] is a consequence of a limited heat flow in the sample but is also due to the constant rise of temperature in the DSC apparatus during a scan.

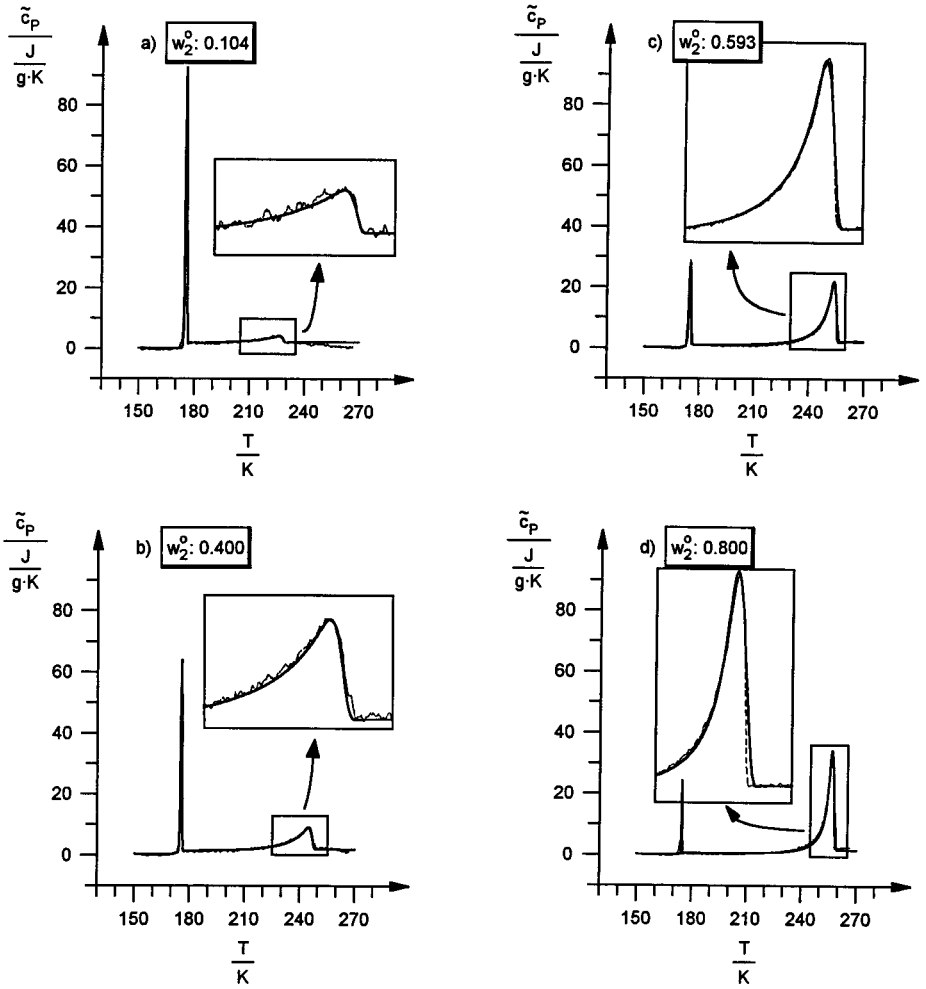

Figure 4. Diagram depicting the calculated DSC curves (solid) and the measured DSC curves (dashed) by using two independent σ parameters for the ascending and descending branches of the underlying Gaussian curves (see text). The concentration dependence of eutectic peak widths ΔT_E has further been taken into account by use of eq 2a.

In the present paper, we turned our attention to simulating this smearing of the DSC curves of the binary model system *n*-hexane/*n*-dodecane. Regardless of the underlying mechanism of heat conduction, the fusion peaks of the binary mixture, appearing subsequently to the eutectic transition, have been based on a superimposition of Gaussian curves of which the widths have been related to those of the respective pure components. Since their fusion peaks reveal an asymmetry in shape—due to a much more steeper descending branch in comparison to its ascending branch—although a Gaussian distribution is perfectly symmetrical, the computed curves are not in a satisfactory agreement with the experimental DSC curves. If, conversely, both branches are separately fitted to the fusion peaks in question, the simulation yields smeared $\tilde{c}_P(T)$ curves that are coincident with the original curves to a large extent.

This implies that smeared DSC curves may satisfactorily be traced by curves attained by superimposing Gaussian curves. Although the present paper has been subject to a model system without any miscibility in the crystalline state, our "smearing procedure" set forth may also be applied to systems with a partial or even complete solid solution behavior.

Acknowledgment. The authors gratefully acknowledge financial support from the Deutsche Forschungsgemeinschaft (DFG). Thanks are also given to Dr. Ralf Jüschke for giving us permission to use his program "WinReg 8.92" for graphical representations.

References and Notes

(1) Müller, A.; Borchard, W. *J. Phys. Chem. B* **1997**, *101*, 4283.
(2) Ehrenfest, P. *Proc. Kon. Akad. Tetenschr. Amsterdam* **1933**, *36*, 153.
(3) Hemminger, W.; Höhne, G. *Calorimetry—Fundamentals and Practice*; Verlag Chemie: Weinheim, 1984; pp 67ff, 89ff.
(4) O'Neill, M. J. *Anal. Chem.* **1964**, *36*, 1238.
(5) Müller, A.; Borchard, W. *J. Phys. Chem. B* **1997**, *101*, 4297.
(6) Illers, K.-H. *Eur. Polym. J.* **1974**, *10*, 911.
(7) Kilian, H. G. *Koll. Z. Polym.* **1965**, *202*, 97.
(8) Landolt-Börnstein, II./4 *Eigenschaften der Materie in ihren Aggregatzuständen: Kalorische Zustandsgrössen*; Springer: Berlin, 1961.